Investigating the onset of energy dissipative processes in heavy ion fusion using MANTEIS

C. C. Seabra[1,*], K.J. Cook[1], J. Buete[1], D. J. Hinde[1], M. Dasgupta[1], S. L. Hayles[1], E. C. Simpson[1], R. Linares[2], H. Lee[1], M. K. Lakelin[1], and T. Tran[1]

[1]Department of Nuclear Physics, Research School of Physics and Engineering, Australian National University, Canberra, ACT 2601, Australia.
[2]Instituto de Física, Universidade Federal Fluminense, 24210-340, Niterói, Rio de Janeiro, Brazil

Abstract.
On the path to fusion, nuclei dissipate their initial kinetic energy into internal excitation, but the understanding of how energy dissipation during the collision affects the resulting fusion cross-sections is still limited.
To investigate energy dissipation in fusion, we are developing a new detector array that measures charge, mass, angle, and excitation energy of scattered particles, called MANTEIS (Multi-ANgle Time and Energy Identification Spectrometer). This detector performs measurements of reflected flux as a function of angle for a given beam energy. These measurements enable us to determine how the projectile and target charge, mass and kinetic energy distributions evolve as nuclei approach each other — effectively measuring the evolution and mechanism of energy dissipation. Here we present the performance and current status of the new detector array.

1 Introduction

Fifteen years have passed since a new superheavy element (SHE) has been synthesised [1]. Until now, all superheavy elements have been produced by fusion, although the mechanisms that influence fusion are far from understood. The synthesis of SHE via fusion is very challenging [2], as it depends on the low probability that one nucleus captures the other as they interact, then forms a compact compound nucleus, equilibrates its mass and charge avoiding quasifission, and finally survives fission to form an evaporation residue.

A key element in characterising the path that nuclei follow towards fusion is the dissipation of energy into internal degrees of freedom. A macroscopic calculation such as with the Coupled-Channels model (CC) cannot reproduce fusion cross-sections below and above the barrier simultaneously [3], as it does not incorporate any energy dissipation mechanism explicitly, hence missing crucial physics. However, more investigation is needed to understand how energy dissipation during the collision affect equilibration processes and the resulting fusion cross-sections.

Nuclei equilibriate mass and charge within the first few zeptoseconds of the collision [4], and fusion cross-sections show a systematic dependence on the identity and structure of the colliding nuclei [5, 6] — indicating that processes that occur before mass equilibration affect fusion probabilities. Also, timescales for charge equilibration and dissipation are faster than mass equilibration [4], indicating that dissipative processes mediated by multinucleon transfer (MNT) processes are important in fusion [7].

The capture process is even more complex than previously thought as, surprisingly, energy dissipation has been found to begin even prior to contact [8]. Multinucleon transfer that happens before capture, as nuclei approach the barrier, change the identity of the nuclei involved, populating high excitation energies and changing the fusion probability significantly [9]. Therefore, by improving our understanding of dissipation mechanisms, we may be able to understand why certain superheavy element reactions are more successful than others.

To investigate this further, we have been developing a new detector system at the Australian National University (ANU). With our new detector array and the Heavy Ion Accelerator Facility at ANU, we aim to probe how the projectile and target nucleus charge, mass, and kinetic energy distributions evolve as they approach each other. We aim to measure the reflected flux (or the failed fusion products) as a function of beam energy, effectively measuring the evolution and mechanism of energy dissipation.

2 Experimental overview

2.1 MANTEIS detector array

Since 2020, we have been developing the concept of a new detector system at the ANU named MANTEIS, the **M**ulti**AN**gle **T**ime and **E**nergy **I**dentification **S**pectrometer. It is designed to determine charge, mass, angle, and excitation energy, for each event by measuring

*e-mail: caroline.seabra@anu.edu.au

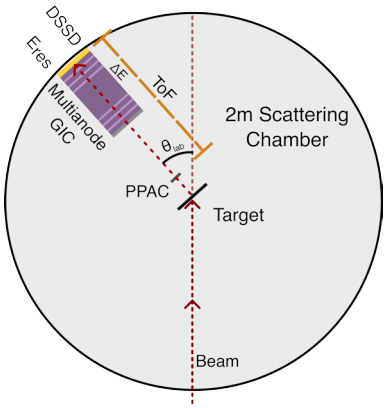

Figure 1. Illustration of the 2-m diameter scattering chamber and the MANTEIS detector array (not to scale). Relative positions of the Parallel Plate Avalanche Counter (PPAC), Gas Ionisation Chamber (GIC), double-sided silicon strip detector (DSSD) are indicated, as well as the quantities measured by each. Beam and scattered particle trajectories are indicated by dashed red lines. The target location inside the chamber is also indicated.

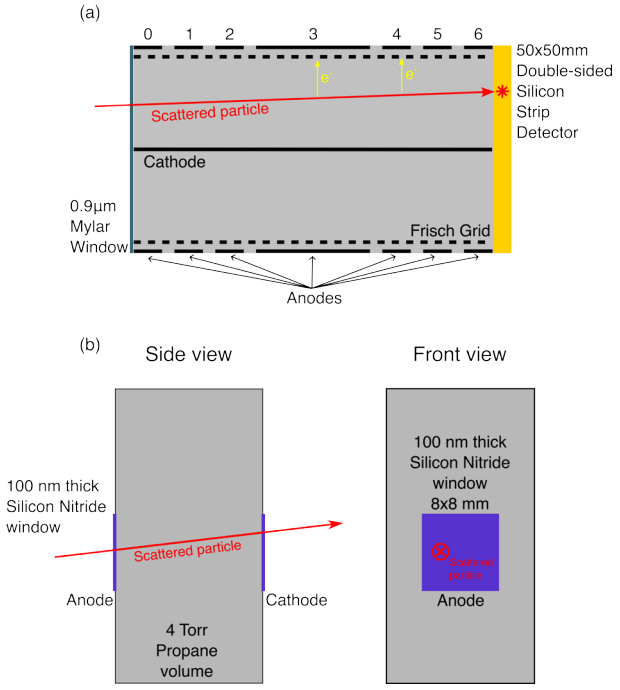

Figure 2. Panel (a): Schematic diagram (not to scale) of the Gas ionisation chamber. The seven-segment anode, cathode, Frisch grid and Mylar window are indicated. A scattered particle trajectory is illustrated by the red arrow, electrons generated by the gas ionisation are illustrated by yellow arrows. Panel (b): Schematic drawing of the Parallel Plate Avalanche Counter (not to scale). 4 Torr propane volume and Silicon Nitride windows are indicated. A scattered particle trajectory is illustrated by the red arrow entering and exiting the detector.

residual energies E_{res}, energy loss ΔE, and time-of-flight ToF.

MANTEIS is composed of a Parallel Plate Avalanche Counter (PPAC) and a Silicon-detector backed Gas Ionisation Chamber (GIC) placed 50 cm apart and mounted on a rotating arm inside a 2 m diameter chamber, as illustrated in Fig. 1. The rotating arm facilitates angular distribution measurements, by varying θ_{lab} without breaking the chamber vacuum. MANTEIS has an angular range of acceptance for particles up to ±1° in θ_{lab}. Except for the silicon detector in the back of the GIC, all detectors were designed and manufactured at ANU.

The GIC consists of a 30 cm long aluminium body with sets of seven anodes on each side, and a cathode parallel to the anodes that run along the middle of the detector. The silicon detector located at the end of the gas volume is a Micron Semiconductors W1 type double-sided silicon strip detector comprising 16 horizontal and vertical segments for residual energy and position measurements. The propane volume inside the GIC is isolated from the 2 m diameter vacuum chamber by a 0.9 μm thick Mylar window with 100 nm Al metallisation, as illustrated in Fig. 2-(a).

The PPAC (illustrated in Fig. 2-(b)) consists of a small aluminium body with two sets of ANU-made 100 nm thick metallised Silicon Nitride windows, that isolate the volume of 4 Torr propane gas from the chamber and hold a uniform bias voltage of 450 V. This results in minimal energy loss and angular straggling, compared to conventional Mylar windows.

After interacting with the target, projectile-like particles will first pass through the PPAC, causing an avalanche of electrons in the gas. The resulting signal, after passing through a charge sensitive preamplifier and fast amplifier, has a 3 ns rise time, making this type of detector suitable for timing application. After travelling further 50 cm, the particle then enters the GIC, losing energy to the gas inside, and reaches the end where a double-sided silicon strip detector (DSSD) is positioned to measure the scattered particle residual energy, time, and position. From the difference in time when a particle passed through the PPAC and stopped in the silicon detector, we obtain its time of flight (ToF). The particle's trajectory is illustrated in Fig. 1.

Therefore, for a given particle, the MANTEIS detector system provides its energy lost in the gas (ΔE), residual energy (E_{res}), and time-of-flight (ToF). The Bethe-Bloch equation (Eq. 1) describes the relation between the energy lost by a particle in a medium and its total energy (E_{total}). Measuring both enables Z identification. With energy and time-of-flight, we can deduce the scattered fragments' mass, and finally with mass, angle and total energy, the excitation energy distributions.

$$\frac{dE}{dx} \propto \frac{MZ^2}{E_{total}} \tag{1}$$

Hence, MANTEIS is designed to be used to measure a variety of processes ranging from elastic and inelastic scattering to transfer and quasifission products.

3 First MANTEIS results: ^{28}Si + ^{248}Cm

In August 2024, the first commissioning experiment was performed. The objective was to measure projectile-like products of the ^{28}Si + ^{248}Cm reaction at E_{lab}

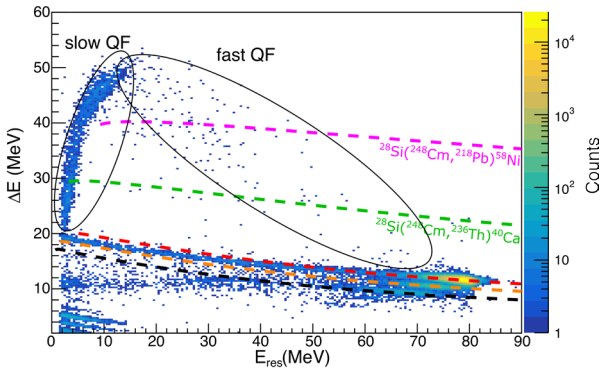

Figure 3. E_{res}-ΔE spectrum for the ^{28}Si + ^{248}Cm system. Fast and slow quasifission outcomes are shown in the figure. Red, yellow and cyan dashed lines are E_{res}-ΔE calculation for ^{28}Si, ^{27}Al and ^{24}Mg isotopes respectively. Magenta and green dashed lines show the E_{res}-ΔE curve when the reaction results in ^{40}Ca and ^{58}Ni, respectively.

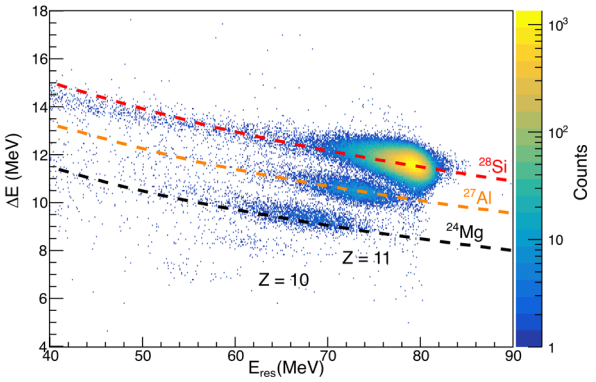

Figure 4. E_{res}-ΔE spectrum for the ^{28}Si + ^{248}Cm system zoomed in the transfer products region. Red, yellow and cyan dashed lines are E_{res}-ΔE calculation for ^{28}Si, ^{27}Al and ^{24}Mg isotopes respectively. Z=11 and Z=10 products are also visible.

= 149.74 MeV (E/V_B = 0.93 [10]), in order to investigate light primary quasifission fragments, eliminating problems due to sequential fission of the heavy fragment [11]. Complementary to this measurement, the sequential fission products for this system were measured with CUBE [12]. Beams were delivered by the 14UD pelletron accelerator at HIAF, ANU.

Fig. 3 shows the E-ΔE spectrum resulting measured at a scattering angle of 135° in the laboratory frame. In the E-ΔE spectrum obtained, it is possible to identify the elastic scattering of ^{28}Si and products of proton stripping leading to Al, Mg, Na and Ne formation. Fig. 4 zooms in on these products.

In Fig. 3, magenta and green dashed lines show E-ΔE curves for ^{58}Ni and ^{40}Ca as ejectiles, respectively. In this spectrum, fragments with mass comparable to ^{58}Ni and ^{40}Ca are results of quasifission, as this process produces energy damped products heavier than transfer reactions. We see two distinct regions in the spectrum where these fragments lie, corresponding to the amount of energy damping that occurs before fragments reseparate. Fast quasifission occurs when the fragments reseparate a few zeptoseconds after capture, while in slow quasifission the fragments' sticking time is longer – exchanging more mass and incurring more energy damping.

The important conclusion from this result is to notice the smooth evolution from the elastic events to fast quasifission to slow quasifission (see Fig. 3), in consequence of the energy that is dissipated through the whole reaction process. With higher statistics, we expect MANTEIS to be useful Z identification in quasifission measurements.

4 Transfer reactions in ^{19}F + ^{120}Sn

In August 2025, we measured transfer products and their excitation energy for the ^{19}F + ^{120}Sn reaction. The objective was to investigate the pairing component of the n-n interaction through the study of transfer reactions induced by heavy ions, by obtaining the angular distribution of the 1- and 2-nucleon stripping and ^{3}He stripping reaction channels. Our detector system MANTEIS has the capability to perform such measurements, as the E_{res}-ΔE spectrum clearly separates different Z, and time-of-flight can distinguish produced isotopes.

At HIAF, a ^{19}F beam at 78 MeV was produced and directed to a 70.8 μg/cm^2 ^{120}Sn target and their reaction products were measured using MANTEIS at 14 different scattering angles ranging from θ_{lab} = 50° to 102°.

Fig. 5-(a) exemplifies an E_{res}-ΔE spectrum for the ^{19}F + ^{120}S reaction products shown at θ_{lab} = 75°. In this figure, distinct transfer products populating a range of excitation energies are shown. Improvements to MANTEIS since 2024 are evident in the excellent Z separation for this mass range. As can be seen in Fig. 5-(a), it's even possible to see bands due to different carbon isotopes only from the E_{res}-ΔE spectrum, showing the good energy resolution we have obtained.

The time-of-flight of the ejectiles were also measured. Fig. 5-(b) illustrates the relation between E_{res} and ToF, for the selection of the locus shown in Fig. 5-(a), and for one pixel in the DSSD, hence the low statistics. Red dotted lines indicate the measured difference in ToF for ^{16}O and ^{18}O isotopes, which is 1.60 ns. Better isotopic separation is possible in the future by improving the time-of-flight and energy determination.

5 Conclusions

Heavy ion fusion is a complex process, especially that leading to SHE formation. It is not very clear how other reaction mechanisms influence the fusion cross-sections, including the dissipation of energy that occurs on the path to fusion. To investigate this problem, at ANU we have been developing a detector system called MANTEIS that can characterise the reaction products as a function of beam energy, probing how the projectile and target mass and charge distributions evolve as the two nuclei approach

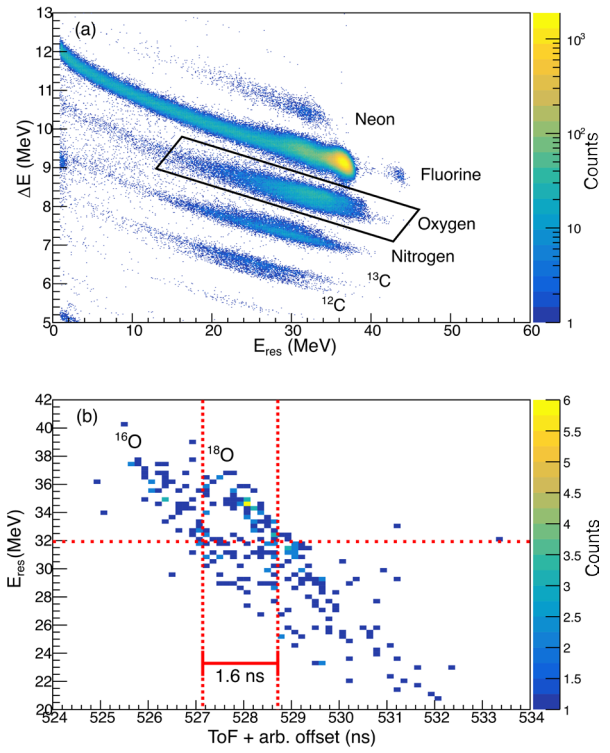

Figure 5. Panel (a): E_{res}-ΔE spectrum for ^{19}F + ^{120}S reaction products at θ_{lab} = 75°. Different Z loci ranging from Neon to Carbon are shown, with distinction of ^{12}C and ^{13}C isotopes. The oxygen locus is selected with the gate shown in black. Panel (b): ToF-E_{res} spectrum for the events of the Oxygen locus selected as shown in panel (a). ^{16}O and ^{18}O isotopes loci are visible. Dark red dotted lines indicate the measured ToF difference for 1.6 ns of ^{16}O and ^{18}O at 32 MeV residual energy.

each other, effectively measuring the evolution of energy dissipation.

For the very first MANTEIS experiment with ^{28}Si + ^{248}Cm, we have seen evidence of a smooth evolution between the elastic scattering products, deep-inelastic collisions and quasifission, due to the dissipation of energy that occurs gradually in these reactions.

We have also used our detector system to measure transfer reactions, and shown we can achieve isotopic separation with the Time-of-Flight measurement. These data are in the process of analysis and the results shown here are preliminary. We expect to be able to use the range of excitation energies seen for the transfer products to investigate the role of energy dissipation for this reaction.

References

[1] Y.T. Oganessian, F.S. Abdullin, P.D. Bailey, D.E. Benker, M.E. Bennett, S.N. Dmitriev, J.G. Ezold, J.H. Hamilton, R.A. Henderson, M.G. Itkis et al., Synthesis of a new element with atomic number Z = 117, Physical Review Letters **104**, 142502 (2010). 10.1103/PhysRevLett.104.142502

[2] J.P. Blocki, H. Feldmeier, W.J. Swiatecki, Dynamical hindrance to compound-nucleus formation in heavy-ion reactions, Nuclear Physics A **459**, 145 (1986). https://doi.org/10.1016/0375-9474(86)90061-8

[3] J.O. Newton, R.D. Butt, M. Dasgupta, D.J. Hinde, I.I. Gontchar, C.R. Morton, K. Hagino, Systematic failure of the Woods-Saxon nuclear potential to describe both fusion and elastic scattering: Possible need for a new dynamical approach to fusion, Physical Review C **70**, 024605 (2004). 10.1103/PhysRevC.70.024605

[4] C. Simenel, K. Godbey, A.S. Umar, Timescales of quantum equilibration, dissipation and fluctuation in nuclear collisions, Physical Review Letters **124**, 212504 (2020). 10.1103/PhysRevLett.124.212504

[5] J. Khuyagbaatar, H.M. David, D.J. Hinde, I.P. Carter, K.J. Cook, M. Dasgupta, C.E. Düllmann, D.Y. Jeung, B. Kindler, B. Lommel et al., Nuclear structure dependence of fusion hindrance in heavy element synthesis, Physical Review C **97**, 064618 (2018). 10.1103/PhysRevC.97.064618

[6] R. du Rietz, E. Williams, D.J. Hinde, M. Dasgupta, M. Evers, C.J. Lin, D.H. Luong, C. Simenel, A. Wakhle, Mapping quasifission characteristics and timescales in heavy element formation reactions, Physical Review C **88**, 054618 (2013). 10.1103/PhysRevC.88.054618

[7] J. Randrup, Mass transport in nuclear collisions, Nuclear Physics A **307**, 319 (1978). https://doi.org/10.1016/0375-9474(78)90621-8

[8] K.J. Cook, D.C. Rafferty, D.J. Hinde, E.C. Simpson, M. Dasgupta, L. Corradi, M. Evers, E. Fioretto, D. Jeung, N. Lobanov et al., Colliding heavy nuclei take multiple identities on the path to fusion, Nature communications **14**, 7988 (2023). https://doi.org/10.1038/s41467-023-43817-8

[9] K.J. Cook, E.C. Simpson, D.C. Rafferty, D.J. Hinde, M. Dasgupta, J. Buete, S.L. Hayles, L. Corradi, M. Evers, E. Fioretto et al., Quantitatively relating multinucleon transfer and fusion, Physics Letters B **865**, 139465 (2025). https://doi.org/10.1016/j.physletb.2025.139465

[10] W.J. Swiatecki, The dynamics of nuclear coalescence or reseparation, Physica Scripta **24**, 113 (1981). 10.1088/0031-8949/24/1B/007

[11] D.Y. Jeung, D.J. Hinde, M. Dasgupta, C. Simenel, E.C. Simpson, K.J. Cook, H.M. Albers, J. Buete, I.P. Carter, C.E. Düllmann et al., Sequential fission and the influence of 208Pb closed shells on the dynamics of superheavy element synthesis reactions, Physics Letters B **837**, 137641 (2023). https://doi.org/10.1016/j.physletb.2022.137641

[12] S.L. Hayles, Reconstructing the first few zeptoseconds of superheavy element synthesis reactions, Honours Thesis (2024)